

Glial Aromatization Decreases Neural Injury in the Zebra Finch (*Taeniopygia guttata*): Influence on Apoptosis

R. D. Wynne and C. J. Saldanha

Department of Biological Sciences, Lehigh University, Bethlehem, PA, USA.

Key words: astrocyte, fadrozole, stroke, oestrogen, pyknosis.

Abstract

Emerging evidence suggests a neuroprotective role for oestrogens following damage to the vertebrate brain. Aromatase (oestrogen synthase) is rapidly transcribed and translated in glial cells around areas of neural damage in several vertebrates. However, the potential neuroprotection afforded by locally up-regulated glial aromatase immediately surrounding the injury remains to be tested. Towards this end, individual birds sustained penetrating mechanical injuries via a needle that contained either vehicle or the aromatase inhibitor fadrozole into contralateral hemispheres. Seventy-two hours later, the size of neural injury (as assessed by the extent of necrotic tissue) and the number of apoptotic cells around the injuries were evaluated. The size of injury in the hemisphere injected with fadrozole was significantly larger than the injury caused by vehicle injection. Furthermore, a greater number of apoptotic nuclei were found around the fadrozole-associated lesion relative to vehicle. Finally, constitutively expressed, neuronal aromatase close to the injury site did not differ between hemispheres. We conclude that local inhibition of glial aromatase immediately around the site of injury plays a neuroprotective role in the songbird brain and this protection involves apoptotic pathways. Local up-regulation of glial aromatase may play a pivotal role in the limitation of secondary damage and/or the acceleration of restorative processes following injury to the vertebrate brain.

Oestrogens mediate many important events in the vertebrate central nervous system (CNS) including neurite outgrowth (1), neuronal migration (2, 3), and perhaps neuronal survival (4). These events likely underlie the pivotal role played by oestrogens in the organization and activation of sexual and other behaviours (5). These effects also include an emerging role for oestrogens in neuroprotection (6).

Premenopausal women appear at a lower risk of stroke than age-matched men, possibly due to higher circulating oestrogen levels (7). In support of this idea, reduced infarction volumes have been reported in female rats compared to males in response to identical neural insults (7). Additionally, oestrogen administration to male rats lowers brain infarction volumes relative to saline treated controls (8). Recently, numerous studies performed both *in vitro* and *in vivo* have found that oestrogens may also play an important role in the protection of neurones against cell damage and death, such as that caused by serum deprivation (9), exposure to glutamate (10) or mechanical injury (11, 12). Taken together, the data strongly suggest a protective role for oestrogens against neural damage. However, the mechanisms of this protection are poorly understood.

Oestrogens such as 17 β -oestradiol are available to the adult CNS from peripheral sites, such as the ovary in females (13), but may also be produced within the brains of both males and females via the expression of aromatase (oestrogen synthase) (14–17). Songbirds (order: Passeriformes) are unique from other homeotherms in that the neural expression of aromatase is particularly abundant and widespread in the telencephalon (18, 19). In particular, aromatase is expressed at high concentrations in several brain areas including the hippocampus, caudomedial and lateral nidopallium and nucleus taeniae (20, 21). In all probability, this abundant expression of aromatase is critical in the provision of oestrogen to telencephalic circuits in species of this order. Because aromatase is extremely low in the telencephalon of adult mammals, songbirds may serve as valuable animal models in understanding the role of local oestrogen provision in the maintenance of neural pathways.

In every homeotherm investigated, the expression of aromatase is limited to the cell bodies and processes of neurones (11, 19, 20, 22). However, under *in vitro* conditions such as primary cell cultures of developing telencephalon, aromatase mRNA, immunoreactive protein and activity is

detectable in glial cells (23–25). Glial aromatase is only detectable in the songbird brain *in vivo* following disruption of the neuropil by injury (11).

As in some rodents (26), a penetrating injury to the zebra finch brain results in a rapid and dramatic increase in aromatase transcription and translation directly surrounding the injury site (11). This increase in aromatase around the injury site may result in high levels of locally synthesized oestrogen, available for the modulation of physiological processes contributing to neuroprotection (6). Studies in which aromatase was systemically inhibited and/or injuries were evaluated in aromatase-knockouts strongly suggest that aromatase may be neuroprotective (26). However, whether (or not) locally up-regulated aromatase has functional consequences upon the extent of neural injury remains to be directly tested.

In the present report, we tested the role of aromatization around neural injury upon: (i) the extent of mechanical injury and (ii) programmed cell death (apoptosis). We report that local inhibition of glial aromatase around the injury site greatly increases the extent of neural damage without an apparent effect on adjacent pools of neuronal aromatase. Furthermore, this effect is accompanied by an increase in apoptotic cells around the injury site.

Materials and methods

Experimental design

Adult male zebra finches (> 90 days of age; Canary Bird Farm, Old Bridge, NJ, USA) were used as subjects in this study. Birds were group-housed in single-sex cages (three per cage) under a 14 : 10 light/dark cycle. The room was maintained at $72 \pm 2^\circ\text{F}$ and food and water were available *ad libitum*.

Each bird served as its own control. The potential role of neural aromatization on injury was tested by injecting fadrozole (27) into one hemisphere and vehicle into the contralateral hemisphere. In three birds, vehicle was first delivered into the right hemisphere followed by fadrozole into the left. In one bird, the fadrozole injection preceded delivery of saline. In the last bird, saline was delivered first into the left hemisphere followed by fadrozole into the right hemisphere. All birds were killed 72 h postinjury. In each bird, we tested the influence of fadrozole on: (i) extent of injury caused by the lesion and injection; (ii) apoptotic cells around the site of injury; and (iii) aromatase expression in glia and neurones. Aromatase protein expression was visualized via immunocytochemistry, and the presence of apoptotic cells was visualized by terminal deoxynucleotidyl transferase biotin-dUTP nick end-labelling (TUNEL). Detailed descriptions of the experimental procedures are presented below.

Surgery: neural injury and delivery of fadrozole

Experimental birds ($n = 5$) were anaesthetized with ketamine/xylazine (0.08 ml per bird with 0.3 and 16 mg/ml ketamine and xylazine) and positioned in a stereotaxic apparatus with the head angled at 45° . The cranium was exposed by midline incision and an 18-G needle was used to create a bilateral craniotomy. Injections were targeted at the entopallial nucleus (previous nomenclature: ectostriatum) 2 mm anterior to the pineal gland and 3 mm lateral to the midline (28). A 50- μl 22-s Hamilton syringe (Hamilton Company, Reno, NV, USA) was positioned at the surface of the brain at an angle of 45° , and lowered 4 mm ventrally where it resided for 60 s. After the initial 60 s, 10 μl of either a 10-mg/ml solution of fadrozole in 0.9% saline or 0.9% saline (vehicle) was injected into one of the two hemispheres. The needle remained in the brain for 60 s following which it was retracted. The scalp was repositioned over the cranium and sealed with Collodion Flexible (EM Science, Gibbstown, NJ, USA). After surgery, the birds recovered from anaesthesia under a heat lamp, and were subsequently used for neuroanatomical analyses 72 h later. The 72-h time point was based upon a previous

report on glial aromatase in the zebra finch that showed robust expression of aromatase mRNA and protein at this time after injury (11).

Tissue preparation

Birds were killed via decapitation and the brain rapidly dissected out and frozen on dry ice. At this time, the abdominal cavity was opened to reveal the testes which were found to be well developed in every bird, suggesting physiological levels of circulating androgen. Coronal frozen sections (20 μm) were cut on a cryostat and thaw-mounted onto superfrost slides. Each slide contained five consecutive sections (total distance sampled was 100 μm) and six alternating sets of sections were collected through the anterior–posterior extent of the brain. Three of these sets were stained with thionin, aromatase, or TUNEL. Other sets served either as replicates or were used for other experiments in the laboratory. Slides were maintained at -80°C until processed for immunocytochemistry or TUNEL.

Thionin histochemistry

Thionin, which stains for the DNA and Nissl granules of neurones and glia, was utilized to determine the total area of the lesion generated by the penetrating needle. This is feasible because the thionin stain around the needle tract is much more intense than that of adjacent healthy neuropil. Within the former, thionin presumably continues to stain Nissl granules and DNA; however, the disrupted and therefore condensed nature of these elements is visible as a more blue and intense stain relative to the surrounding tissue. Sections were fixed in 4% paraformaldehyde (pH = 7.34) for 10 min, washed in distilled water for 1 min and stained with thionin as previously reported (20). Sections were then dehydrated through graded alcohols (70, 95, 95, 100, 100%), cleared with xylene, and coverslipped.

TUNEL histochemistry

The TUNEL Apoptosis Detection Kit was purchased from Upstate Biotechnology (Charlottesville, VA, USA). Briefly, sections were fixed in 4% paraformaldehyde (pH = 7.34) for 10 min and washed in 0.1 M phosphate buffer saline (PBS) $\times 1$ for 30 min at room temperature. Sections were then incubated with terminal deoxynucleotidyl transferase (TdT) buffer (30 mM Tris-HCl buffer, pH 7.4, containing 140 mM sodium cacodylate, 1 mM cobalt chloride) for 10 min followed by incubation in TdT end-labelling cocktail containing TdT buffer, biotin-dUTP, and TdT at a 90 : 5 : 5 ratio for 120 min at 37°C . Once incubation in the cocktail was complete, the reaction was terminated by immersing the sections in $1 \times$ Termination Buffer (0.1 M TRIS-HCl buffer containing 30 mM NaCl and 30 mM sodium citrate) for 5 min at room temperature. Sections were once again washed with 0.1 M PBS for 10 min, and then incubated in a 1 : 200 avidin–biotin complex (Vectastain, Vector Laboratories, Burlingame, CA, USA) in 0.3% PBT for 60 min at room temperature. Sections were then washed in 0.1 M PBS $\times 1$ for 45 min, and incorporated biotin was visualized using the Vector SG substrate kit (Vector Laboratories) for peroxidase. Following the colour reaction, sections were washed once for 5 min in 0.1% PBT, dehydrated through graded alcohols (70, 95, 95, 100, 100%), cleared with xylene, and coverslipped.

Aromatase immunocytochemistry

The immunocytochemistry protocol has been described previously (21). Sections were fixed in 4% paraformaldehyde (pH = 7.34) for 10 min and then washed 3×5 min in 0.1 M phosphate buffer to eliminate excess aldehydes. The sections were then immersed in 0.036% H_2O_2 for 10 min to neutralize endogenous peroxidases. Sections were treated with 10% normal goat serum (Vector Laboratories) in 0.3% Triton X100 in phosphate buffer (PBT) for 60 min at room temperature. For primary antibody treatment, mounted sections were incubated with a 1 : 2500 polyclonal aromatase antibody for 24 h at room temperature. Once primary incubation was complete, sections were washed 3×5 min with 0.1% PBT and treated with a 1 : 200 biotinylated goat anti-rabbit IgG (Vector Laboratories) in 0.3% PBT for 60 min. Following secondary incubation, sections were washed (3×5 min) in 0.1% PBT and then incubated in a 1 : 200 avidin–biotin complex (Vectastain) in 0.3% PBT for 60 min at room temperature. After washing the sections 3×5 min in 0.1% PBT, aromatase immunoprotein was visualized using 0.03% diaminobenzidine containing 0.8 μM nickel sulphate and 0.9 μM cobalt chloride activated with 0.001% H_2O_2 . Following the colour reaction, sections

were washed once for 5 min in 0.1% PBT, dehydrated through graded alcohols (70, 95, 95, 100, 100%), cleared with xylene, and coverslipped. Slides were examined by means of the Nikon eclipse E1000M (Nikon, Tokyo, Japan) to determine the presence and distribution of immunoprotein.

Data collection and statistical analysis

The potential effects of aromatase-inhibition via the delivery of fadrozole were assessed on: (i) size of injury and (ii) apoptotic cells around the injury site. In addition, to validate the efficacy of fadrozole-administration, we measured aromatase expression in glia around the injury site (injury-induced aromatase) and in neurones in the ventromedial nucleus of the hypothalamus (VMN; constitutive neuronal aromatase).

Effect of fadrozole on size of injury

To describe the effect of fadrozole on size of injury, we measured the total area of the lesion on thionin-stained sections and on sections stained for aromatase. Image analysis (NIH Image; <http://rsb.info.nih.gov/nih-image/>) was used to render a digitized image of the injury site under low magnification for area measurements. Area measurements were performed by two experimenters, one of whom was blind to the experimental condition of the animals. Between 10 and 15 images of injury were captured per bird and the area of the needle tract was measured. We computed the: (i) area of injury per section and (ii) the total area of injury by summing the injury area over the number of sections analysed within each slide and multiplying by 600 [the distance (in μm) between successive slides within each series]. Analysis of variance (ANOVA) with Tukey–Kramer post-hoc tests were used to compare the injury in the hemisphere injected with fadrozole to that in the hemisphere injected with vehicle.

Effect of fadrozole on injury-induced apoptosis

The effect of fadrozole upon injury-induced apoptosis was measured to identify potential mechanisms whereby glial aromatization ameliorates the extent of neural injury. Evaluation of injury-induced programmed cell death was performed by measuring: (i) the density of apoptotic cells along the entire length of the neural injury and (ii) the density of apoptotic cells immediately surrounding the tip of the neural injury alone. We selected sections containing different portions of neural injury induced by the needle (i.e. the tip, the shaft, and the point of insertion into the brain) by referencing sections previously processed via immunocytochemistry and thionin. The total number of apoptotic nuclei around the injury was not evaluated. Multiple random samples (10 fields around each injury per bird) of a 64 000 μm^2 area from the point of insertion, shaft, and tip of the needle tract were averaged within each hemisphere and bird. Images of sections labelled via TUNEL were captured at $\times 200$ magnification and the number of positively stained apoptotic nuclei was counted by two individuals, both of whom were blind to the experiment.

These same observers also measured the distance of apoptotic nuclei from the edge of the necrotic zone. In low-power images, the distance from the necrotic margin to approximately 25 cells furthest from the injury (18–42 per injury) was measured and averaged within hemisphere and bird. Data were compared between fadrozole- and saline-associated injuries using ANOVA and post hoc Tukey–Kramer tests.

Effect of fadrozole on aromatase-expression

The effect of fadrozole on aromatase expression around the injury was measured to determine the efficacy of drug delivery. Correspondingly, the spatial extent (diffusion of delivered drug around the injection site) of this potential effect was estimated by comparing constitutive neuronal aromatase-expression across both hemispheres. We measured: (i) the relative intensity of immunoprotein within individual immunoreactive glia and neurones and (ii) the density of immunoreactive cell bodies (number of immunoreactive astrocytes per unit area). Hereafter, we use the terms ‘intensity’ for the amount of immunoprotein on digitized images and ‘density’ for the number of immunoreactive cells per unit area.

The intensity of immunoprotein on digitized images of the area directly surrounding the injury was quantified as an indirect measure of aromatase expression. Immunoprotein of individual astrocytic cells was digitized at high magnification ($\times 400$) and the intensity of immunostain in 75–100 astrocytes immediately surrounding the injury. The limits of the intensity were set by the digitizing software utilized (NIH Image) ranging from 0 (white) to 255 (black).

The astrocytes sampled included only those with clear, unstained nuclei. The intensity of adjacent neuropil lacking visible immunostain was also measured as an index of background intensity. The relative intensity of immunostain was normalized within each subject by either subtracting the background from that of specific immunostain, or by dividing that of specific immunostain by background. Two individuals who were blind to the study performed all density measurements. Identical procedures were used to measure the intensity of aromatase neurones in the VMN.

The intensity of aromatase expression was compared by two-way ANOVA with type of cell (glial versus neuronal) and treatment (fadrozole versus saline) as the main variables. Post-hoc Tukey–Kramer (main variables) and least square means (interaction) tests were used to evaluate sources of systematic variation.

Results

In the present experiment, the aromatase-inhibitor, fadrozole (27) and vehicle injections were injected into contralateral hemispheres within each subject. Thus, each subject served as its own control. We assessed: (i) the extent of injury caused by delivery of the drug; (ii) the density and intensity of apoptotic cells immediately surrounding the injury; (iii) the density and intensity of injury-dependent glial aromatase expression around the needle-tract; and (iv) the density and intensity of constitutive neuronal aromatase expression in the VMN, a locus approximately 3 mm away from the entoptallic nucleus.

Effect on neural injury size

The injury caused by penetration of the drug-delivery needle was measured on each side of the brain in all sections with a visible tract (Fig. 1A). The area of injury on each section and the total injury (sum of the area of injury over all sections processed) was compared between hemispheres that received either fadrozole or vehicle.

The size of injury was consistently greater in the hemisphere that received fadrozole compared to vehicle (Fig. 1). Specifically, the size of injury per section on sections stained with thionin was greater around the tract receiving fadrozole [$F(1,4) = 6.956$; $P = 0.0298$] as was the total size of injury over all sections with a visible injury tract [$F(1,4) = 10.439$; $P = 0.0319$] (Fig. 1B). The absolute size of injury did not differ between sections stained with thionin or aromatase in that total injury and injury per section measures were similar in magnitude. Specifically, comparable measures were obtained from sections processed with aromatase immunocytochemistry for total injury [$F(1,8) = 8.263$; $P = 0.0188$] as well as injury per section [$F(1,8) = 22.401$; $P = 0.0091$].

Effect on apoptosis

Programmed cell death was analysed on each side of the brain by two separate measures: (i) the density of TUNEL labelled cells along the entire length of the injury tract and (ii) the density of TUNEL labelled cells at the tip of the needle.

The density of apoptotic cells along the entire length of the injury tract did not differ between hemispheres that received fadrozole or vehicle [554 ± 108 versus 422 ± 116 ; fadrozole versus vehicle; $F(1,7) = 0.682$; $P = 0.4363$]. However, within individual subjects the fadrozole associated

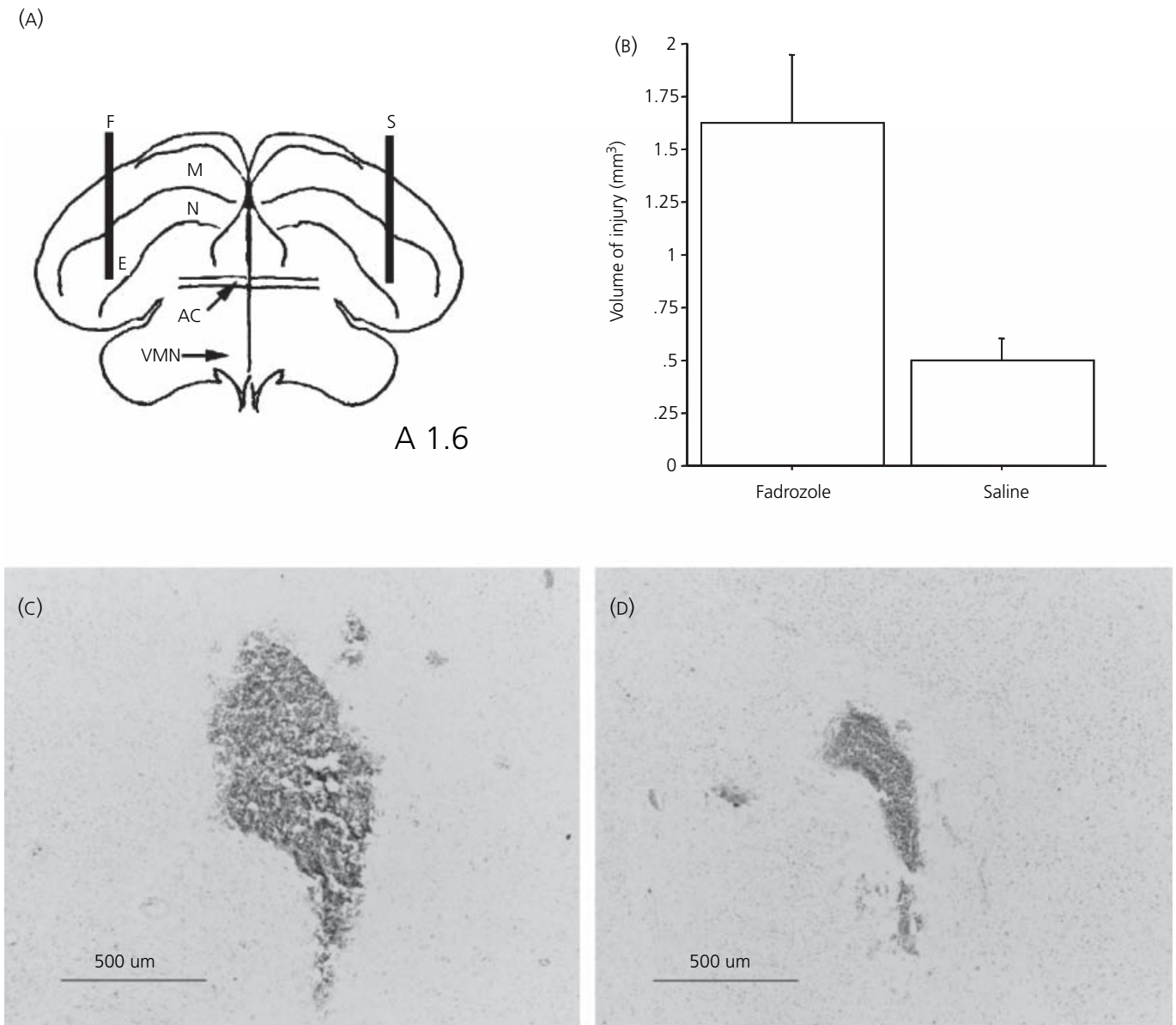


FIG. 1. (A) The experimental design is depicted in schematic. The coronal section shows injection of fadozole (F) or saline (S) into the entopallium (E) in contralateral hemispheres of individual birds. M, Mesopallium; N, nidopallium; AC, anterior commissure; VMN, ventromedial nucleus of the hypothalamus. The anteroposterior position of the sections is depicted (28). The injury caused by penetration of the drug-delivery needle was measured on each side of the brain in all sections with a visible injury tract. The total injury (sum of the area of injury over all sections processed), is shown in (B). The injury is visible as necrotic tissue in thionin-stained sections through the site of fadozole (C) and saline (D) injection. Photomicrographs are from the same experimental animal.

injury consistently showed greater numbers of apoptotic nuclei relative to vehicle. Therefore, we re-evaluated the number of apoptotic cells located at the tip of the needle only (Fig. 2A) and found that the density of apoptotic cells in the hemisphere injected with fadozole was significantly higher than the hemisphere injected with vehicle [$F(1,4) = 11.627$; $P = 0.0270$] (Fig. 2B).

The distance of apoptotic nuclei from the edge of the necrotic zone was not statistically different between fadozole- and saline-induced injuries (225 ± 26 versus 204 ± 19 ; fadozole versus saline; $P = 0.54$).

Effect on injury-induced aromatase expression

The expression of aromatase in glia was consistently higher in the hemisphere that received fadozole in comparison to vehicle for intensity measures (Fig. 4). In particular, the intensity of aromatase positive glia was higher around the tract receiving fadozole when the relative intensity of aromatase immunoprodukt was normalized within each subject by dividing the background intensity from that of specific immunostain [$F(1,8) = 10.190$; $P = 0.0122$]. Similar results were observed when the relative intensity of aromatase immuno-

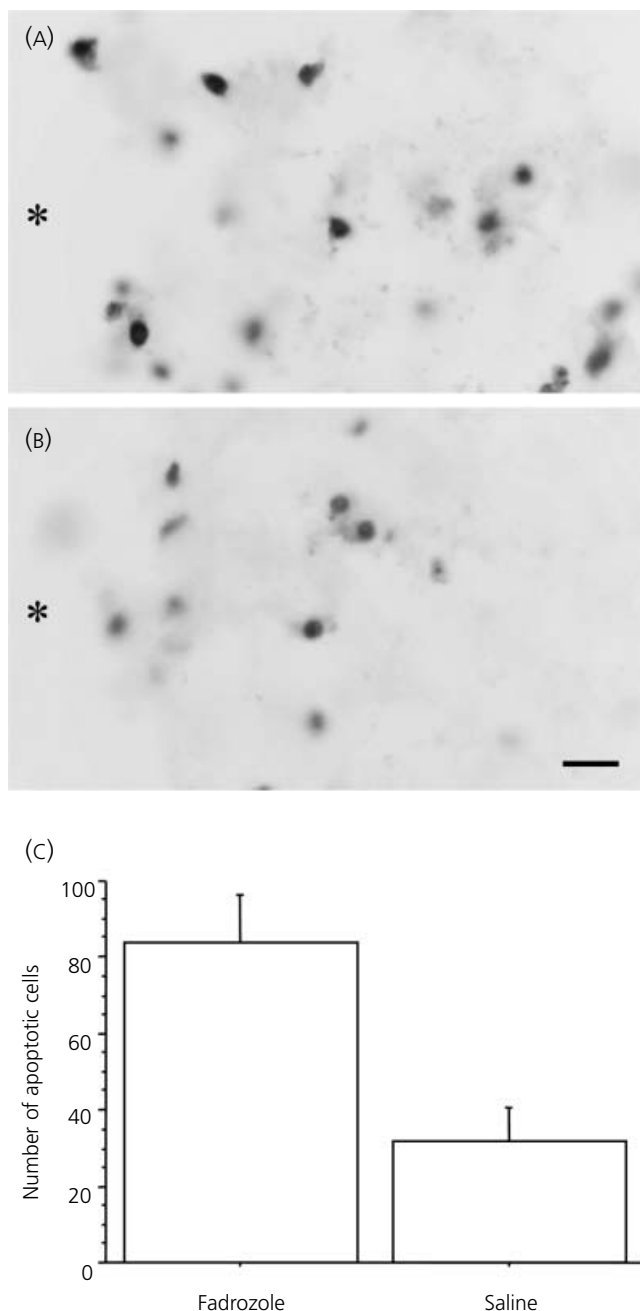


FIG. 2. High-power photomicrographs depicting apoptotic nuclei adjacent to the fadrozole (A) or saline (B) associated needle tracts (asterisks) in an individual, representative subject. Scale bar = 10 μ m for both panels. (C) Histogram of the difference in the number of apoptotic cells at the tip of the injection needle between fadrozole- and saline-associated injuries ($P < 0.05$).

product was normalized within each subject by subtracting the background intensity from that of specific immunostain [(F(1,8) = 10.861; $P = 0.0472$]. Because both measures generated similar trends in the relative intensity of staining of aromatase immunoproduct, we hereafter present values normalized by dividing the background intensity from that of specific immunostain. The density (number of cells per unit area) of aromatase immunostained reactive glia surrounding

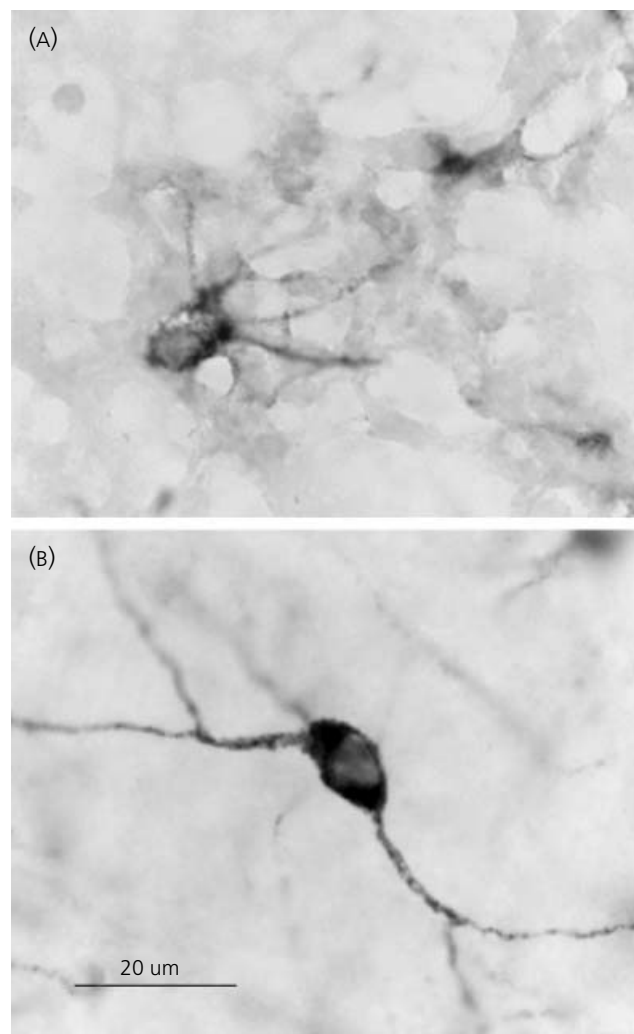


FIG. 3. High-power photomicrograph showing the morphological difference between aromatase-expressing glia around the injury site (A) and aromatase-expressing neurones (B) in the zebra finch brain. Magnification is identical in both panels.

the fadrozole injection was not different in comparison to the saline injection [F(1,8) = 0.028; $P = 0.8709$] (data not shown).

Effect on constitutive neuronal aromatase expression

The intensity of 100 aromatase positive neuronal cells (Fig. 3B) and the density of aromatase positive neuronal cells were measured and compared between hemispheres that received either fadrozole or vehicle.

The expression of aromatase in neuronal cells was comparable between both hemispheres for all intensity and density measurements (Fig. 4). Specifically, the intensity of aromatase positive neurones was indistinguishable between the hemisphere of the brain that received the fadrozole injection in comparison to the saline injection [(F(1,8) = 0.857; $P = 0.3902$; 1.91 ± 0.072 versus 1.83 ± 0.045 ; fadrozole versus saline]. Similarly, the density of aromatase positive neurones was nearly identical for each side of the brain that received the fadrozole injection or the saline

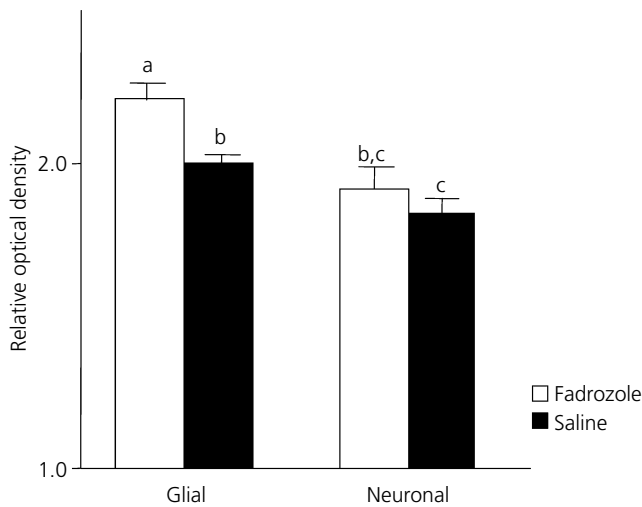


FIG. 4. Histogram of relative optical density of aromatase expression in glial (injury-induced) and neuronal (constitutive) cells in fadrozole versus saline injected hemispheres. Columns with different letters are significantly different ($P < 0.05$).

injection [$F(1,8) = 16.397$; $P = 0.5829$; 42.5 ± 4.9 versus 41.6 ± 2.4 ; fadrozole versus saline].

Discussion

In the current study, we examined the role of aromatization around neural injury on two separate measures: (i) the extent of mechanical injury and (ii) programmed cell death (apoptosis). We found that local inhibition of glial aromatase around the injury site greatly increases the extent of neural damage (Fig. 1) without an apparent effect on adjacent pools of neuronal aromatase (Fig. 4). Additionally, this effect is accompanied by an increase in apoptotic cells around the fadrozole-associated injury site (Fig. 2). These data suggest that inactivation of aromatase results in increased vulnerability to neural insult *in vivo*. Additionally, the neuroprotective function of aromatase is mediated via pathways that include (but are perhaps not limited to) apoptotic signalling cascades as evidenced by the greater number of cells undergoing apoptosis around the tip of the needle delivering fadrozole.

As described in previous studies, local oestrogen synthesis may increase around neural insult due to the up-regulation of glial aromatase, suggesting a protective role for the enzyme aromatase and its biosynthetic product oestrogen (6, 8, 11, 21, 26, 29). Therefore, it may be predicted that, by locally inhibiting aromatase activity, the neuroprotective functions of aromatase would be decreased. As described, local injection of fadrozole increased the extent of injury relative to saline approximately two-fold, suggesting that up-regulated aromatase plays a crucial role in neuroprotection. This observation is in excellent agreement with other studies reporting that global inhibition of aromatase activity via peripheral delivery of fadrozole resulted in decreased survival of hilar neurones relative to animals treated with vehicle (26). Moreover, neural injury is potentiated in aromatase knockout mice

relative to homozygous and heterozygous wild-types (26). The present study extends these findings to suggest that discrete inhibition of local, injury-induced aromatase results in an increase in the magnitude of injury. To our knowledge, this is the first study that directly manipulates local aromatase activity levels immediately surrounding neural injury.

Although we cannot unequivocally define the extent of diffusion of administered fadrozole, the data suggest that the treatment was indeed restricted to the area immediately surrounding the injury. The efficacy of fadrozole treatment was assessed by measuring the immunoprotein intensity in injury induced glia. Aromatase positive glia around the injury created by fadrozole were darker than glia around vehicle injection (Fig. 4), indicating a decrease in aromatase activity because fadrozole causes an increase in aromatase mRNA and protein levels (30). Furthermore, to test whether the injection of fadrozole remained local to the injury site, we measured the intensity of staining in aromatase positive neurones in the VMN, approximately 3 mm distal to the site of injury. The staining intensity of neurones containing aromatase on the side injected with fadrozole was not significantly different from the neurones containing aromatase on the side that received saline (Fig. 4), supporting the idea that injected fadrozole remained local to the injury site. Finally, the intensity of staining of aromatase positive glia regardless of injection type was equivalent or higher than that of aromatase positive neuronal cells located in the VMN, suggesting that up-regulated injury induced glial aromatase may be physiologically relevant because studies have shown aromatase expressed in the hypothalamus is critical in the regulation of sexually dimorphic behaviours in several animal models (31). We have no direct knowledge of the time-course of aromatase activity inhibition achieved in the current experiment. However, our treatments and observations are consistent with other studies describing the dissociation between fadrozole-induced activity inhibition and protein expression up-regulation (30).

Previous studies have demonstrated that the up-regulation of aromatase protein following neural injury occurs in reactive astrocytes (11, 21, 26). Similar results are presented in the current report. Unfortunately, classical markers for glia do not work well in songbirds (11); thus, the identification of injury-induced aromatase is limited to morphological criteria. As shown in Fig. 3(A,B), the morphology of glial cells around the neural injury is distinct from aromatase-positive neuronal cells constitutively expressed in the VMN. To further support this idea, neural injuries were created in the entopallium (Fig. 1A), which is an area of the avian brain that lacks constitutively expressing aromatase positive neuronal cells. These data reinforce the idea that glial cells assist in neuroprotection of the vertebrate brain.

In the present report, programmed cell death around the fadrozole-associated injury exceeded that around vehicle-associated injury. However, we believe that apoptosis may account for only some of the total cell loss occurring after injury. The number of apoptotic nuclei around the entire fadrozole-associated injury was 125% of that around vehicle injections. However, the size of injury around the fadrozole

injection was 200% of that around vehicle. This suggests that apoptotic pathways account for some, but not all, of the loss of viable cells around the injury tract. Indeed, previous research suggests that both apoptosis and necrosis contribute to cell death following neural injury (32). Furthermore, excitotoxic injury of the rodent visual cortex reveals pyknotic pathways as assessed by Fluoro-Jade staining (33). Taken together, the current findings suggest that several signalling pathways mediate cell death as well as survival following traumatic brain injury.

Locally up-regulated aromatase may increase oestrogen levels surrounding the injury. Oestradiol may protect the brain by actions on traditional intranuclear oestrogen receptors (ER) or via nongenomic pathways (34). This action may involve several cell types including neurones, astrocytes, endothelia and microglia (34). Indeed, previous studies have found an increase in ER- α (ER α) in reactive astrocytes and androgen receptor (AR) in microglia after brain injury in the rat (29). Others have demonstrated that ER α , and not ER β , is a critical mechanistic link in mediating the protective effects of estradiol in a mouse model of brain injury (35). The up-regulation of steroid receptors following brain injury may be important in the activation of various growth- and survival-promoting factors such as fibroblast growth factor, insulin-like growth factor-1, transforming growth factor- β , and connective tissue growth factor (29). We do not know which, or even if, steroid receptors are up-regulated around injury in the songbird. These hypotheses are currently being tested in our laboratory and may indicate crucial mechanisms whereby oestrogens increase neural survival and promote the reorganization of the adult vertebrate brain.

Acknowledgements

We thank Joe Oberlander and Luckshman Coomaringam for assistance with data collection. This research was supported by NIH NS 042767 (C.J.S.).

Accepted 27 May 2004

References

- Toran-Allerand CD, Hashimoto K, Greenough WT, Saltarelli M. Sex steroids and the development of the newborn mouse hypothalamus and preoptic area in vitro. III. Effects of estrogen on dendritic differentiation. *Brain Res* 1983; **283**: 97–101.
- Hidalgo A, Barami K, Iversen K, Goldman SA. Estrogens and non-estrogenic ovarian influences combine to promote the recruitment and decrease the turnover of new neurons in the adult female canary brain. *J Neurobiol* 1995; **27**: 470–487.
- Burek MJ, Nordeen KW, Nordeen EJ. Estrogen promotes neuron addition to an avian song-control nucleus by regulating post-mitotic events. *Brain Res Dev Brain Res* 1995; **85**: 220–224.
- Arnold AP, Gorski RA. Gonadal steroid induction of structural sex differences in the central nervous system. *Annu Rev Neurosci* 1984; **7**: 413–442.
- McEwen BS. Invited review: estrogens effects on the brain: multiple sites and molecular mechanisms. *J Appl Physiol* 2001; **91**: 2785–2801.
- Garcia-Segura LM, Azcoitia I, DonCarlos LL. Neuroprotection by estradiol. *Prog Neurobiol* 2001; **63**: 29–60.
- Barrett-Connor E, Bush TL. Estrogen and coronary heart disease in women. *Jama* 1991; **265**: 1861–1867.
- Toung TJ, Traystman RJ, Hurn PD. Estrogen-mediated neuroprotection after experimental stroke in male rats. *Stroke* 1998; **29**: 1666–1670.
- Green PS, Gridley KE, Simpkins JW. Estradiol protects against beta-amyloid (25–35)-induced toxicity in SK-N-SH human neuroblastoma cells. *Neurosci Lett* 1996; **218**: 165–168.
- Mize AL, Shapiro RA, Dorsa DM. Estrogen receptor-mediated neuroprotection from oxidative stress requires activation of the mitogen-activated protein kinase pathway. *Endocrinology* 2003; **144**: 306–312.
- Peterson RS, Saldanha CJ, Schlinger BA. Rapid upregulation of aromatase mRNA and protein following neural injury in the zebra finch (*Taeniopygia guttata*). *J Neuroendocrinol* 2001; **13**: 317–323.
- Callard GV, Kunz TH, Petro Z. Identification of androgen metabolic pathways in the brain of little brown bats (*Myotis lucifugus*): sex and seasonal differences. *Biol Reprod* 1983; **28**: 1155–1161.
- MacLusky NJ, Philip A, Hurlburt C, Naftolin F. Estrogen formation in the developing rat brain: sex differences in aromatase activity during early post-natal life. *Psychoneuroendocrinology* 1985; **10**: 355–361.
- Balthazart J, Foidart A, Surlemont C, Harada N. Distribution of aromatase-immunoreactive cells in the mouse forebrain. *Cell Tissue Res* 1991; **263**: 71–79.
- Schlinger BA, Arnold AP. Circulating estrogens in a male songbird originate in the brain. *Proc Natl Acad Sci USA* 1992; **89**: 7650–7653.
- Roselli CE, Resko JA. The distribution and regulation of aromatase activity in the central nervous system. *Steroids* 1987; **50**: 495–508.
- Schlinger BA, Arnold AP. Brain is the major site of estrogen synthesis in a male songbird. *Proc Natl Acad Sci USA* 1991; **88**: 4191–4194.
- Schlinger BA. The activity and expression of aromatase in songbirds. *Brain Res Bull* 1997; **44**: 359–364.
- Shen P, Schlinger BA, Campagnoni AT, Arnold AP. An atlas of aromatase mRNA expression in the zebra finch brain. *J Comp Neurol* 1995; **360**: 172–184.
- Saldanha CJ, Tuerk MJ, Kim YH, Fernandes AO, Arnold AP, Schlinger BA. Distribution and regulation of telencephalic aromatase expression in the zebra finch revealed with a specific antibody. *J Comp Neurol* 2000; **423**: 619–630.
- Garcia-Segura LM, Wozniak A, Azcoitia I, Rodriguez JR, Hutchison RE, Hutchison JB. Aromatase expression by astrocytes after brain injury: implications for local estrogen formation in brain repair. *Neuroscience* 1999; **89**: 567–578.
- Shen P, Campagnoni CW, Kampf K, Schlinger BA, Arnold AP, Campagnoni AT. Isolation and characterization of a zebra finch aromatase cDNA. *in situ hybridization reveals high aromatase expression in brain. Brain Res Mol Brain Res* 1994; **24**: 227–237.
- Schlinger BA, Amur-Umarjee S, Shen P, Campagnoni AT, Arnold AP. Neuronal and non-neuronal aromatase in primary cultures of developing zebra finch telencephalon. *J Neurosci* 1994; **14**: 7541–7552.
- Freking F, Ramachandran B, Schlinger BA. Regulation of aromatase, 5 alpha- and 5 beta-reductase in primary cell cultures of developing zebra finch telencephalon. *J Neurobiol* 1998; **36**: 30–40.
- Saldanha CJ, Popper P, Micevych PE, Schlinger BA. The passerine hippocampus is a site of high aromatase: inter- and intraspecies comparisons. *Horm Behav* 1998; **34**: 85–97.
- Azcoitia I, Sierra A, Veiga S, Honda S, Harada N, Garcia-Segura LM. Brain aromatase is neuroprotective. *J Neurobiol* 2001; **47**: 318–329.
- Wade J, Schlinger BA, Hodges L, Arnold AP. Fadrozole, a potent and specific inhibitor of aromatase in the zebra finch brain. *Gen Comp Endocrinol* 1994; **94**: 53–61.
- Stokes TM, Leonard CM, Nottebohm F. The telencephalon, diencephalon, and mesencephalon of the canary, *Serinus canaria*, in stereotaxic coordinates. *J Comp Neurol* 1974; **156**: 337–374.
- Garcia-Ovejero D, Veiga S, Garcia-Segura LM, DonCarlos LL. Glial expression of estrogen and androgen receptors after rat brain injury. *J Comp Neurol* 2002; **450**: 256–271.
- Harada N, Honda SI, Hatano O. Aromatase inhibitors and enzyme stability. *Endocr Relat Cancer* 1999; **6**: 211–218.
- Schlinger BA. The activity and expression of aromatase in songbirds. *Brain Res Bull* 1997; **44**: 359–367.

- 32 Newcomb JK, Zhao X, Pike BR, Hayes RL. Temporal profile of apoptotic-like changes in neurons and astrocytes following controlled cortical impact injury in the rat. *Exp Neurol* 1999; **158**: 76–88.
- 33 Gilliams-Francis KL, Quaye AA, Naegele JR. PARP cleavage, DNA fragmentation, and pyknosis during excitotoxin-induced neuronal death. *Exp Neurol* 2003; **184**: 359–372.
- 34 Wise PM, Dubal DB, Wilson ME, Rau SW, Bottner M. Minireview: neuroprotective effects of estrogen—new insights into mechanisms of action. *Endocrinology* 2001; **142**: 969–973.
- 35 Dubal DB, Zhu HYUJ, Rau SW, Shughrue PJ, Merchenthaler I, Kindy MS, Wise PM. Estrogen receptor alpha, not beta, is a critical link in estradiol-mediated protection against brain injury. *Proc Natl Acad Sci USA* 2001; **98**: 1952–1957.